J. Biochem. 2012;152(1):37–43 doi:10.1093/jb/mvs044

JB THE JOURNAL OF BIOCHEMISTRY

Reactive oxygen species production and activation mechanism of the rice NADPH oxidase OsRbohB

Received November 24, 2011; accepted February 28, 2012; published online April 23, 2012

Shinya Takahashi[1,*], Sachie Kimura[1], Hidetaka Kaya[1], Ayako Iizuka[1], Hann Ling Wong[2,*], Ko Shimamoto[2] and Kazuyuki Kuchitsu[1,†]

[1]Department of Applied Biological Science, Tokyo University of Science, Noda, 278-8510 Chiba and [2]Graduate School of Biological Sciences, Nara Institute of Science and Technology, Ikoma, 630-0192 Nara, Japan

*Present addresses: Shinya Takahashi, Graduate School of Frontier Sciences, The University of Tokyo, Kashiwa, 277-8562 Chiba, Japan; Hann Ling Wong, Department of Biological Science, Universiti Tunku Abdul Rahman, Jalan Universiti, Bandar Barat, 31900 Kampar, Perak, Malaysia.
First three authors contributed equally to this work.

†To whom correspondence should be addressed. Tel: +81 4 7122 9404, Fax: +81 4 7123 9767, email: kuchitsu@rs.noda.tus.ac.jp

Reactive oxygen species (ROS) produced by plant NADPH oxidases (NOXes) are important in plant innate immunity. The *Oryza sativa respiratory burst oxidase homologue B* (*OsRbohB*) gene encodes a NOX the regulatory mechanisms of which are largely unknown. Here, we used a heterologous expression system to demonstrate that OsRbohB shows ROS-producing activity. Treatment with ionomycin, a Ca^{2+} ionophore, and calyculin A, a protein phosphatase inhibitor, activated ROS-producing activity; it was thus OsRbohB activated by both Ca^{2+} and protein phosphorylation. Mutation analyses revealed that not only the first EF-hand motif but also the upstream amino-terminal region were necessary for Ca^{2+}-dependent activation, while these regions are not required for phosphorylation-induced ROS production.

Keywords: calcium ion (Ca^{2+})/EF-hand motif/NADPH oxidase (NOX)/reactive oxygen species (ROS)/respiratory burst oxidase homologue (Rboh).

Abbreviations: Ca^{2+}, calcium ion; CA, calyculin A; DPI, diphenylene iodonium; HEK, human embryonic kidney; NOX, NADPH oxidase; PCR, polymerase chain reaction; Rboh, respiratory burst oxidase homologue; ROS, reactive oxygen species.

Plants have several defence systems to cope with biotic stress. Rapid production of reactive oxygen species (ROS), termed an oxidative burst, is one such defence mechanism against attacks by pathogens (*1*). ROS induce cross-linking of cell walls, cell death, expression of defence genes and propagation of rapid systemic signalling.

Plant ROS are produced by the NADPH oxidase (NOX), respiratory burst oxidase homologue (Rboh). The rice *Oryza sativa RbohA* (*OsRbohA*) gene was previously isolated as a homologue of $gp91^{phox}$/NOX2, which is a catalytic subunit of the mammalian NOX complex (*2*). Since then, *Rboh* genes have been isolated from various plant species including *Arabidopsis*, tobacco and potato (*3–6*).

Plant Rboh proteins are predicted to contain six conserved transmembrane helices, and cytosolic FAD- and NADPH-binding domains in the carboxy (C)-terminal region, which is homologous to NOX2. Unlike NOX2, however, all plant Rboh proteins have an extended amino (N)-terminal region that includes two EF-hand motifs (*7*). NOX1–4 have no EF-hand motif, whereas human NOX5 has four (three canonical and one non-canonical) in its N-terminal extension (*8*). The EF-hand motif is composed of a typical helix-loop-helix structural unit: two α-helices bridged by a Ca^{2+}-binding loop (*9*, *10*).

Nine *OsRboh* (*OsRbohA–I*) genes have been identified in the rice genome. The transient expression of *OsRbohB* was previously shown to enhance basal ROS production in *Nicotiana benthamiana* (*11*); however, it remains unknown whether the ROS-producing activity of OsRbohB is mediated by NOX. Moreover, the activation mechanisms of OsRbohB involving the two EF-hand motifs and the N-terminal region are unclear.

To understand the ROS-producing activity and activation mechanism of OsRbohB, we employed a heterologous expression system using human embryonic kidney (HEK) 293T cells. HEK293T cells have low ROS-producing activity due to an absence of NOX2 and NOX5 activity. This feature allows us to monitor exogenous NOX activity quantitatively in real time (*12*, *13*) as was reported for *Arabidopsis thaliana* Rboh (AtRboh) (*14*, *15*).

This study demonstrated ROS-producing activity and the activation mechanism of OsRbohB. We further analysed the functions of the regulatory domains in the N-terminal cytoplasmic region and revealed that not only the EF-hand motif but also the upstream N-terminal region was required for Ca^{2+}-dependent but not phosphorylation-dependent activation.

Materials and Methods

Plasmid constructs

OsRbohB complementary DNA (cDNA; AK065117) was amplified by the polymerase chain reaction (PCR) with the following primers containing *Bam*HI restriction sites (underlined): OsRbohB-orf-F (5′-CGGGATCCGCTGACCTGGAAGCAGGCAT-3′) and OsRbohB-orf-R (5′-CGGGATCCTTAGAAGTTCTCCTTGTG

GA-3′). The amplified fragment was digested with *Bam*HI and inserted into the corresponding sites of the pcDNA3.1 (–) vector (Invitrogen). OsRbohB was then fused with a 3×FLAG epitope tag at its 5′-end. We also generated mutants of 3×FLAG:OsRbohB containing D242A, G247A, E253Q, D286A, G291A and D297N mutations, and a 3×FLAG:Δ226-OsRbohB deletion mutant (Δ1–226 a.a.).

Cell culture and transfection

HEK293T cells were maintained at 37°C in 5% CO_2 in Dulbecco's modified Eagle's medium nutrient mixture F-12 HAM (Sigma) supplemented with 10% fetal bovine serum. HEK293T cells were transiently transfected with 100 ng of the indicated plasmid or an empty vector pcDNA3.1 (–) using Opti-MEM (Invitrogen) and GeneJuice transfection reagent (Novagen) according to the manufacturer's protocol.

Measurement of ROS production

ROS production was measured by the peroxidase-dependent luminol-amplified chemiluminescence technique according to a previously described method (*14*, *15*). Measurements were made in buffer containing 1.26 mM Ca^{2+} (unless otherwise stated). To mobilize Ca^{2+} uptake, 1 μM ionomycin (Calbiochem) was applied to cells. Chemiluminescence was measured every minute at 37°C using a microplate luminometer (Centro LB960; Berthold Technologies). ROS production was expressed as relative luminescence units per second (RLU/s). Data are presented as an average of three samples from a representative experiment. This experiment was independently replicated more than three times. Protein expression was detected by Western blotting with an anti-FLAG antibody (M2; Sigma). Comparable protein loading was confirmed by blotting with a β-actin antibody as a control.

Results

Ca^{2+}-dependent ROS-producing enzymatic activity of OsRbohB

We used a heterologous expression system based on HEK293T cells to examine the ROS-producing enzymatic activity of OsRbohB. Cells were transfected with *OsRbohB* or empty vector as a negative control. OsRbohB was fused with a FLAG epitope tag. Given that OsRbohB contains two EF-hand motifs within its N-terminal region (*16*), we hypothesized that it is activated by Ca^{2+}. We therefore added 1 μM ionomycin, which is a Ca^{2+} ionophore that induces Ca^{2+} influx into cells. Ionomycin rapidly and transiently induced ROS production in *OsRbohB*-transfected cells but not in empty vector-transfected cells (Fig. 1A), suggesting that Ca^{2+} induces the ROS-producing enzymatic activity of OsRbohB.

To determine whether ionomycin-induced ROS production is attributable to the NOX activity of OsRbohB, we pretreated transfected cells with diphenylene iodonium (DPI), which inhibits NOX activity. DPI successfully abolished ionomycin-induced ROS production in a dose-dependent manner (Fig. 1B), indicating that ROS production is mediated by the NOX activity of OsRbohB.

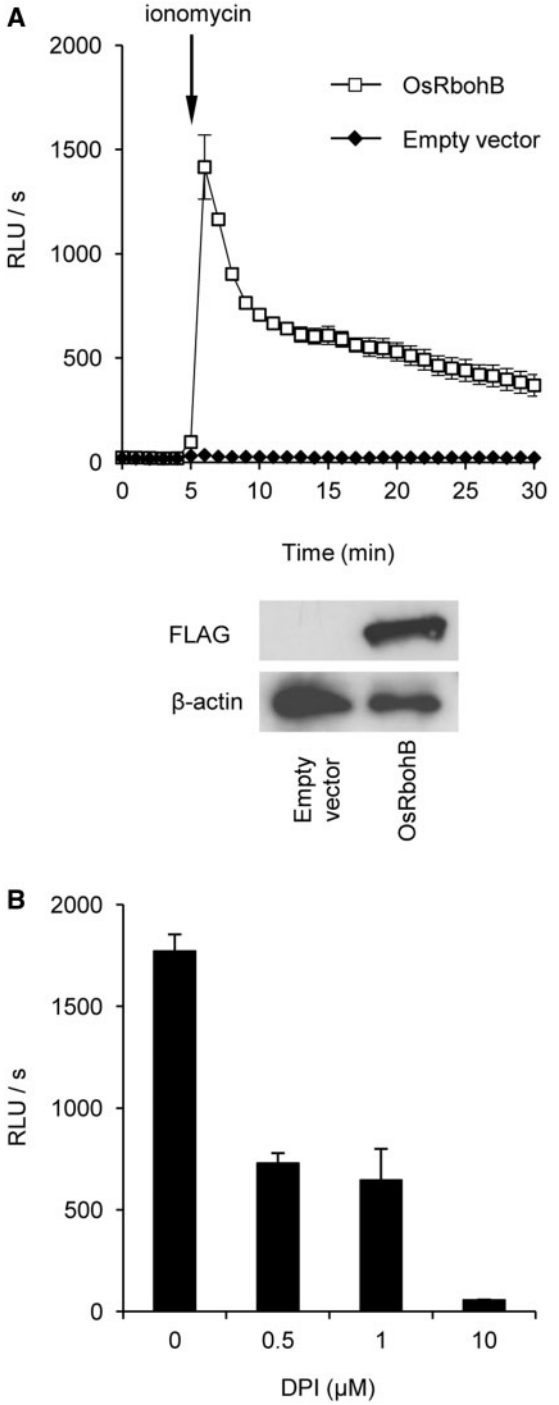

Fig. 1 Ionomycin-induced ROS production by OrRbohB *via* NOX enzymatic activity. (A) HEK293T cells were transiently transfected with *FLAG:OsRbohB* (open squares) or empty vector (closed diamonds). Baseline measurements were made for 5 min, after which 1 μM ionomycin was added. ROS production was measured as RLU/s. Protein expression was detected by Western blotting. (B) *FLAG:OsRbohB*-transfected cells were treated with the indicated concentrations of DPI for 20 min. Ionomycin was then added to the cells. The highest peaks of each RLU/s are plotted.

A role for the putative EF-hand motifs in the Ca^{2+}-induced activation

We generated OsRbohB mutants carrying point mutations in the first EF-hand motif, EF-1 (D242A, G247A and E253Q at X, G and –Z, respectively), and the second EF-hand motif, EF-2 (D286A, G291A and D297N at X, G and –Z, respectively), to determine the role of the two EF-hand motifs in the ionomycin-induced ROS-producing activity of OsRbohB (Fig. 2A). We predicted that these substitutions would greatly reduce the Ca^{2+} affinity of the EF-hand motif as they included changes to the critical six amino acids (X, Y, Z, –Y, –X and –Z) contained within the Ca^{2+}-binding loop and involved in Ca^{2+}

chelation (*9*, *10*). Moreover, glycine provides the bend in the secondary structure of the EF-hand loop (*10*). Indeed, ionomycin-induced ROS production by OsRbohB was largely abolished by each of the three mutations in EF-1 (Fig. 2B–D). Conversely, the three mutations in EF-2 caused no change in ROS-producing activity (Fig. 2E–G). The D286A-OsRbohB mutant showed much higher ROS-producing activity than wild type (Fig. 2E), whereas the G291A and D297N mutations had little effect on ionomycin-induced ROS production by OsRbohB (Fig. 2F and G). These results suggest that ionomycin-induced ROS production requires the Ca^{2+}-affinity of EF-1 but not that of EF-2.

A role for the upstream N-terminal region in the Ca^{2+}-induced activation

The N-terminal region of OsRbohB contains two EF-hand-like domains, EF-like 1 and EF-like 2, which are predicted from the structural analysis but not from the amino acid sequence (Fig. 3A) (*16*). To examine the roles of the N-terminal region in ROS production, we generated the N-terminal deletion mutant, Δ226-OsRbohB (Fig. 3A), which completely abolished the ionomycin-induced ROS-producing activity of OsRbohB (Fig. 3B). This indicates that not only the EF-hand motif but also the N-terminal region is necessary to activate the Ca^{2+}-dependent ROS production of OsRbohB.

Protein phosphorylation-induced activation and its requirement of the regulatory domains

In cultured rice cells, the phosphatase inhibitor calyculin A (CA) induces ROS production (*17*), which is inhibited by DPI (*18*). It also enhances the protein phosphorylation of AtRbohD protein in HEK293T cells (*14*). To test the effect of CA on ROS production by OsRbohB, we added CA to *OsRbohB*-transfected or empty vector-transfected HEK293T cells. CA slowly and continuously induced ROS production in *OsRbohB*-transfected cells, but not in empty vector-transfected cells, suggesting that protein phosphorylation activates OsRbohB (Fig. 4A).

Both ionomycin and CA induce ROS production (Figs 1A and 4A), which suggests that Ca^{2+} and protein phosphorylation activate the ROS-producing activity of OsRbohB. To understand the relationship between Ca^{2+} and protein phosphorylation in the activation of OsRbohB, we examined CA-induced ROS production by OsRbohB in Ca^{2+}-free buffer. We also analysed the E253Q-OsRbohB and Δ226-OsRbohB mutants that were not activated by ionomycin (Figs 2D and 3B). CA was found to induce ROS production by not only OsRbohB but also E253Q-OsrbohB and Δ226-OsRbohB even in Ca^{2+}-free buffer (Fig. 4B). These results suggest that protein phosphorylation-induced ROS production by OsRbohB is independent of Ca^{2+}, EF-hand regions and the N-terminal region (1–226 a.a.).

Although CA also induced ROS production by E253Q-OsRbohB and Δ226-OsRbohB, their activity was reduced in comparison with OsRbohB (Fig. 4B). Previous study of OsRbohB suggests that EF-hand motif has a very weak affinity for the C-terminal region independently of Ca^{2+} (*16*). The EF-hand mutation in E253Q-OsRbohB may have had an effect on this affinity. The upstream N-terminal region (1–226 a.a.) contains several predicted phosphorylation sites (Fig. 5). Accordingly, protein phosphorylation-induced ROS production by Δ266-OsRbohB may have been reduced.

Synergistic activation of OsRbohB by protein phosphorylation and Ca^{2+}

We next analysed the interrelationship between CA and ionomycin on the activation of OsRbohB. When we added CA and ionomycin to *OsRbohB*-transfected HEK293T cells, the ROS-producing activity was significantly enhanced compared with the activation from either CA or ionomycin alone (Fig. 6). This result suggests that OsRbohB is synergistically activated by Ca^{2+} and protein phosphorylation.

Discussion

The present study analysed the activation mechanism of OsRbohB using a heterologous expression system based on HEK293T cells. We quantitatively monitored ROS production derived from OsRbohB in real time and observed that it was mediated by NOX activity (Fig. 1). OsRbohB was activated by ionomycin *via* its EF-hand motif (Fig. 2) and by CA (Fig. 4A), as well as by both together (Fig. 6). These results suggest that OsRbohB is activated by Ca^{2+} and protein phosphorylation and is synergistically activated by both.

In mammalian NOX5, protein phosphorylation was shown to facilitate enzyme activation at lower levels of $[Ca^{2+}]_{cyt}$ (*19*). Protein phosphorylation of OsRbohB might, therefore, contribute to the Ca^{2+} affinity of the EF-hand motif, leading to the observed synergistic activation by protein phosphorylation and Ca^{2+}. This synergistic activation also resembles that of AtRbohC/ROOT HAIR DEFECTIVE 2 (RHD2) and AtRbohD (*14*, *15*), suggesting that the mechanism might be conserved among rice, *Arabidopsis* and other plant species.

We also demonstrated that EF-1 mutations abolished ionomycin-induced ROS production (Fig. 2B–D). Recent structural analysis of OsRbohB showed that EF-1 bound Ca^{2+}, while the E253A mutant in EF-1 did not bind Ca^{2+} (*16*). These results suggest that EF-1 is critical for Ca^{2+}-dependent activation of OsRbohB. Our present study found, conversely, that EF-2 mutations, which were predicted to reduce Ca^{2+} affinity of the EF-hand motif, did not reduce ionomycin-induced ROS production (Fig. 2E–G). A previous structural study showed that OsRbohB forms a homodimer structure in which EF-1 of one molecule interacts with EF-2 of another in a domain-swapping manner (*16*). The amino acid sequence of EF-2 significantly deviates from the canonical one, and no bound Ca^{2+} was found in EF-2 (*16*). Thus, EF-2 might contribute more to dimer stabilization than to Ca^{2+} affinity during Ca^{2+}-dependent ROS production.

Ionomycin-induced ROS production by OsRbohB was shown to require not only the EF-hand region

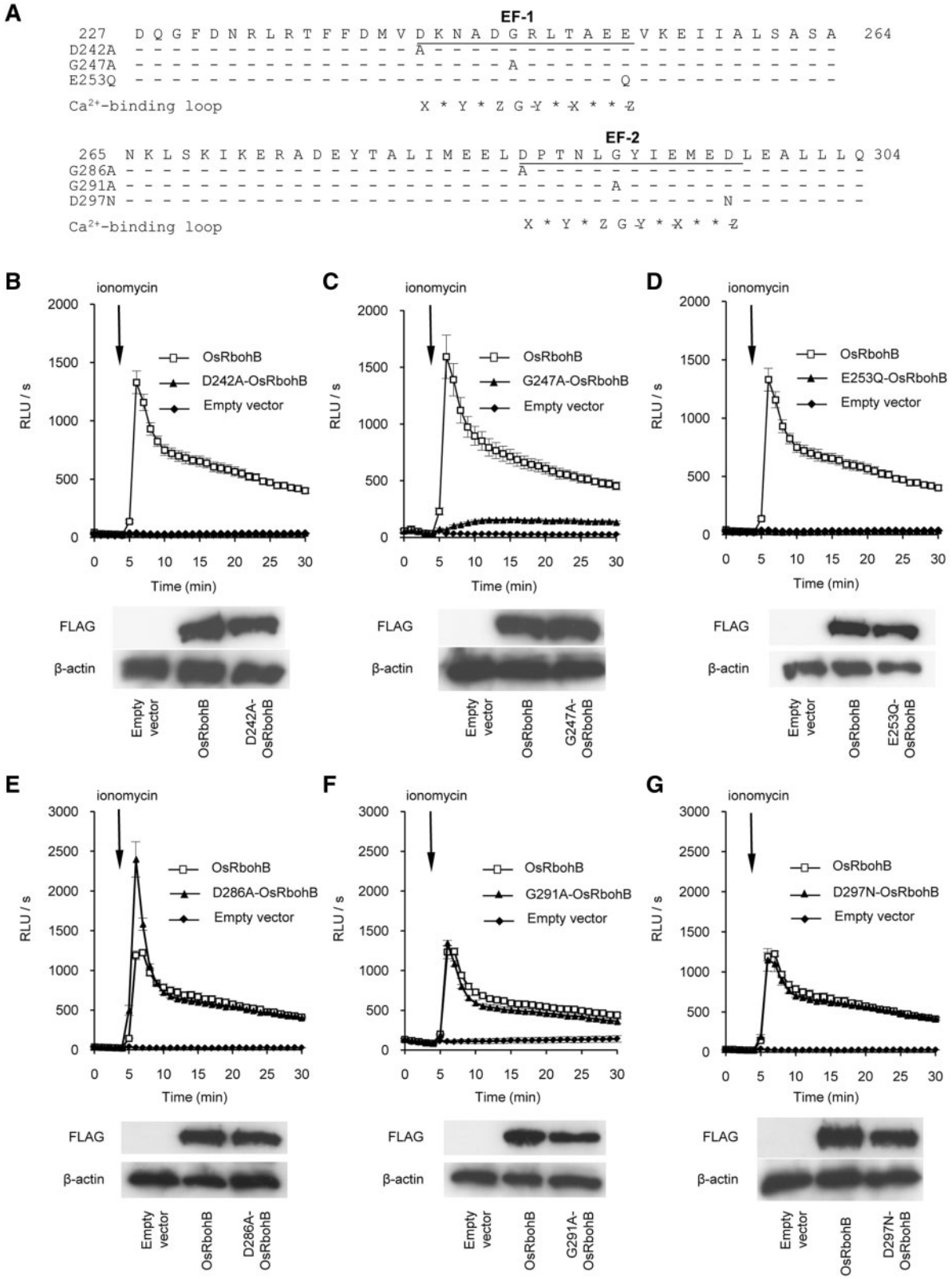

Fig. 2 Role of the two EF-hand motifs on ionomycin-induced ROS-producing activity of OsRbohB. (A) Amino-acid sequence of OsRbohB EF-hand regions (227–304 a.a.). The consensus Ca^{2+}-binding loop is shown: first (X), third (Y), fifth (Z), seventh (–Y), ninth (–X) and twelfth (–Z) = Ca^{2+} ligand; sixth (G) = glycine. (B–G) HEK293T cells were transiently transfected with *FLAG:OsRbohB* (open squares), empty vector (closed diamonds) or the indicated plasmids (closed triangles): (B) *FLAG:D242A-OsRbohB*; (C) *FLAG:G247A-OsRbohB*; (D) *FLAG:E253Q-OsRbohB*; (E) *FLAG:D286A-OsRbohB*; (F) *FLAG:G291A-OsRbohB* and (G) *FLAG:D297N-OsRbohB*. Baseline measurements were made for 5 min, after which 1 μM ionomycin was added. ROS production was measured as RLU/s. Protein expression was detected by Western blotting.

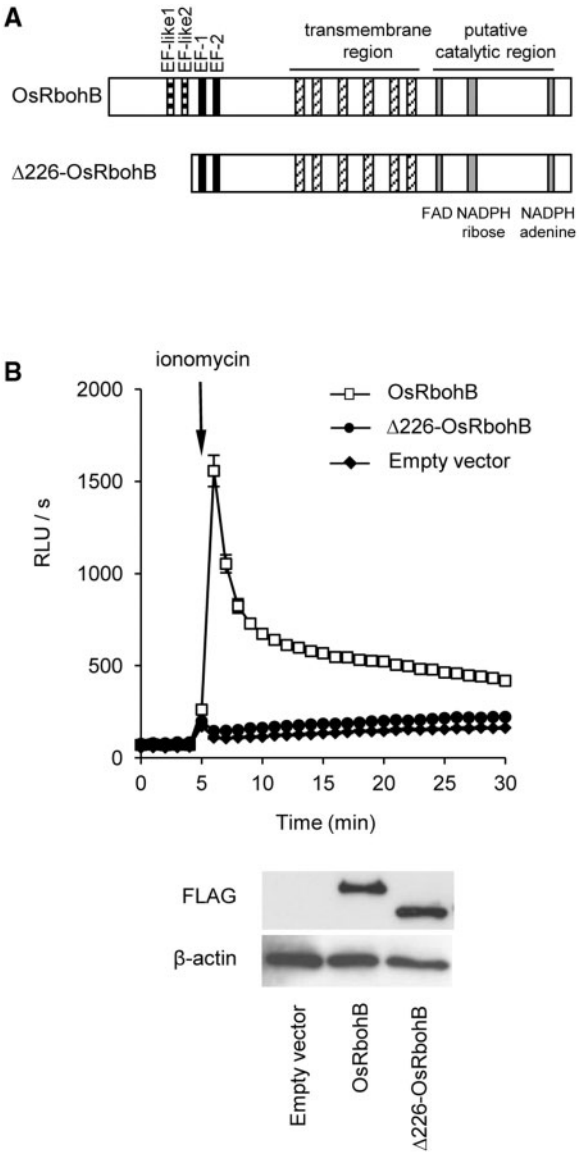

Fig. 3 Activity determination of OsRbohB protein with deleted N-terminus (1–226 a.a.). (A) Schematic representation of OsRbohB and N-terminal deletion mutant (Δ226-OsRbohB). OsRbohB contains two EF-hand-like motifs (EF-like 1 and EF-like 2), two EF-hand motifs (EF-1 and EF-2), six transmembrane domains and a catalytic region (FAD- and NADPH-binding domains). (B) HEK293T cells were transiently transfected with *FLAG:OsRbohB* (open squares), *FLAG:Δ226-OsRbohB* (closed circles) or empty vector (closed diamonds). Baseline measurements were made for 5 min, after which 1 μM ionomycin was added. ROS production was measured as RLU/s. Protein expression was detected by Western blotting.

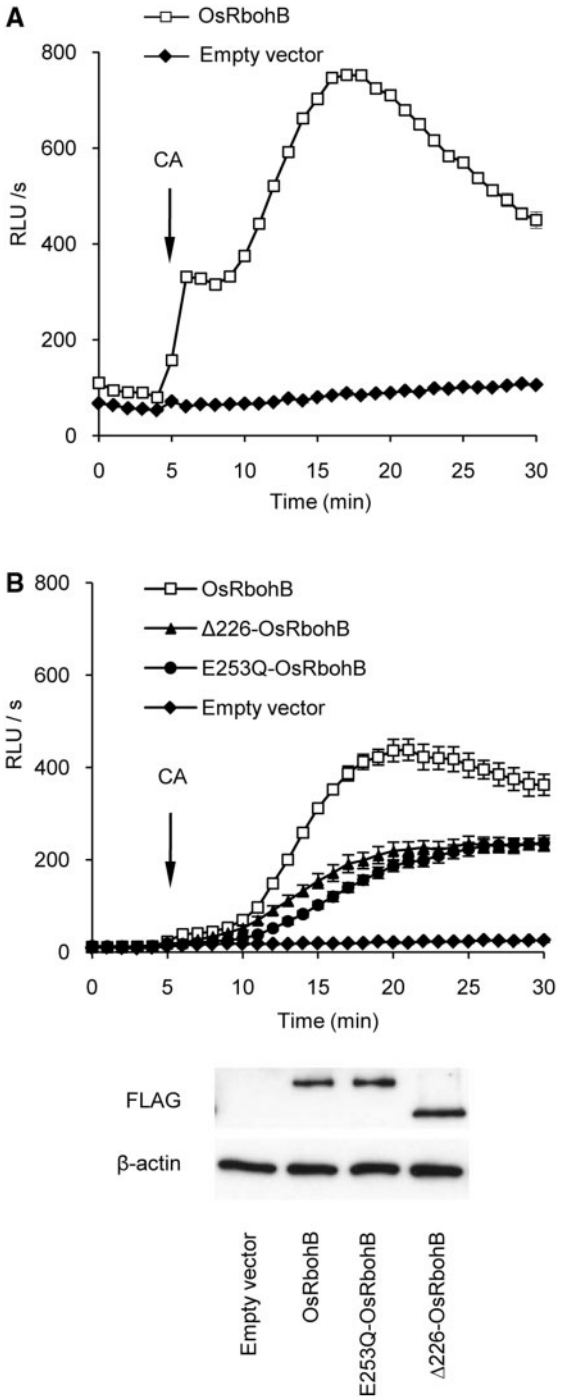

Fig. 4 CA-induced ROS-producing activity of OsRbohB. (A) HEK293T cells were transiently transfected with *FLAG:OsRbohB* (open squares) or empty vector (closed diamonds). Baseline measurements were made for 5 min, after which 0.1 μM CA was added. (B) HEK293T cells were transiently transfected with *FLAG:OsRbohB* (open squares), *FLAG:Δ226-OsRbohB* (closed triangles), *FLAG:E253Q-OsRbohB* (closed circles) or empty vector (closed diamonds). Protein expression was detected by Western blotting. Measurements were made in buffer with (in A) or without (in B) Ca^{2+}.

but also the upstream N-terminal region (1–226 a.a.), suggesting that the latter contains unknown regulatory domains for Ca^{2+}-dependent ROS production. EF-like 1 and EF-like 2 are putative regulatory domains (Fig. 3A), the amino-acid sequences of which differ from that of the canonical EF-hand motif, but which together form a domain that preserves the structural feature of the EF-hand motif (*16*). It is conceivable that the four EF-hand motifs (EF-1, EF-2, EF-like 1 and EF-like 2) of OsRbohB may coordinately function for Ca^{2+}-dependent ROS-producing activity, much like the four EF-hands motifs of mammalian NOX5, which shows Ca^{2+}-dependent ROS-producing activity (*8*). It is also possible that other unknown domains present in the N-terminal region function in Ca^{2+}-dependent ROS-producing activity.

Fig. 5 Predicted phosphorylation sites in OsRbohB. Amino acid sequence of the upstream N-terminal region (1–226 a.a.) and the C-terminal region (590–905 a.a.) of OsRbohB are underlined by straight and broken lines, respectively. The predicted phosphorylated serine (S) or threonine (T) by the NetPhos 2.0 server (http://www.cbs.dtu.dk/services/NetPhos/) are shown by gothic letters.

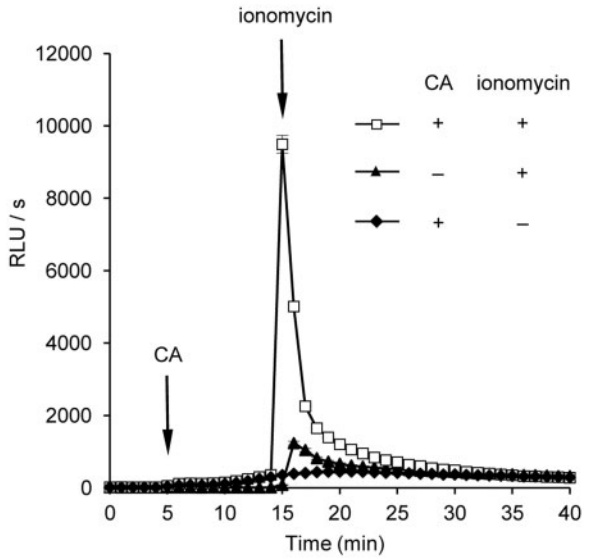

Fig. 6 Synergistic activation by CA and ionomycin. HEK293T cells were transiently transfected with *FLAG:OsRbohB*. Baseline measurements were made for 5 min, then measurements were taken with 0.1 μM CA followed 10 min later by ionomycin addition (open squares), with ionomycin addition alone (closed triangles) or with CA addition alone (closed diamonds).

Although CA induced the ROS-producing activity of OsRbohB, similar to ionomycin, the temporal pattern of ROS production was clearly different. ROS production induced by CA was slow and continuous, whereas that induced by ionomycin was rapid and transient (Figs 4 and 1A). Both of the EF-hand motifs and the N-terminal region (1–226 a.a.) were required for ionomycin-induced ROS production, whereas both were dispensable for CA-induced ROS production, suggesting that there are at least two distinct mechanisms for the activation of OsRbohB, in which different domains are involved. Ca^{2+} binding to the EF-hand motif of the OsRbohB N-terminal region induces a conformational change (*16*); this indicates that such a Ca^{2+}-dependent conformational change leads to OsRbohB activation. In addition to the EF-hand motifs, further upstream N-terminal region has been shown to play a critical role in Ca^{2+}-dependent activation. Alternatively, protein phosphorylation might induce conformational changes in the C-terminal region of OsRbohB. In C-terminal region of NOX5, four phosphorylation sites are phosphorylated, leading to activation of NOX5 (*19*). The NetPhos 2.0 server (http://www.cbs.dtu.dk/services/NetPhos/) predicted that 18 Ser/Thr residues were phosphorylation sites in the C-terminal region (590 a.a. onward) of OsRbohB (Fig. 5). It should be important to dissect the roles of various regulatory domains in Ca^{2+}-dependent and phosphorylation-dependent activation in Rboh proteins in various plant species.

Acknowledgements

We thank Ms. Eriko Senzaki, Ms. Haruka Hishinuma, Ms. Aya Imai, Ms. Hitomi Nibori, Ms. Tomoko Kawarazaki, Mr. Masataka Michikawa and Mr. Ryo Nakajima for technical support; Dr. Takashi Oda and Dr. Toshiyuki Shimizu for valuable suggestions and Dr. Takamitsu Kurusu for critical reading.

Funding

Ministry of Education, Culture, Sports, Science and Technology (MEXT), Japan (a grant-in-aid for Scientific Research on Innovation Area to H.K. (No. 21200068) and to K.K. (No. 21117516)).

Conflict of Interest

None declared.

References

1. Doke, N., Miura, Y., Sanchez, L.M., Park, H.J., Noritake, T., Yoshioka, H., and Kawakita, K. (1996) The oxidative burst protects plants against pathogen attack: mechanism and role as an emergency signal for plant bio-defence—a review. *Gene* **179**, 45–51
2. Groom, Q.J., Torres, M.A., Fordham-Skelton, A.P., Hammond-Kosack, K.E., Robinson, N.J., and Jones, J.D. (1996) *rbohA*, a rice homologue of the mammalian $gp91^{phox}$ respiratory burst oxidase gene. *Plant J.* **10**, 515–522
3. Torres, M.A., Onouchi, H., Hamada, S., Machida, C., Hammond-Kosack, K.E., and Jones, J.D. (1998) Six *Arabidopsis thaliana* homologues of the human respiratory burst oxidase ($gp91^{phox}$). *Plant J.* **14**, 365–370
4. Keller, T., Damude, H.G., Werner, D., Doerner, P., Dixon, R.A., and Lamb, C. (1998) A plant homolog of the neutrophil NADPH oxidase $gp91^{phox}$ subunit gene encodes a plasma membrane protein with Ca^{2+} binding motifs. *Plant Cell* **10**, 255–266
5. Yoshioka, H., Sugie, K., Park, H.J., Maeda, H., Tsuda, N., Kawakita, K., and Doke, N. (2001) Induction of plant gp91 phox homolog by fungal cell wall, arachidonic acid, and salicylic acid in potato. *Mol. Plant Microbe Interact.* **14**, 725–736
6. Yoshioka, H., Numata, N., Nakajima, K., Katou, S., Kawakita, K., Rowland, O., Jones, J.D., and Doke, N. (2003) *Nicotiana benthamiana* $gp91^{phox}$ homologs *NbrbohA* and *NbrbohB* participate in H_2O_2 accumulation and resistance to *Phytophthora infestans*. *Plant Cell* **15**, 706–718
7. Torres, M.A. and Dangl, J.L. (2005) Functions of the respiratory burst oxidase in biotic interactions, abiotic

stress and development. *Curr. Opin. Plant Biol.* **8**, 397–403

8. Banfi, B., Tirone, F., Durussel, I., Knisz, J., Moskwa, P., Molnar, G.Z., Krause, K.H., and Cox, J.A. (2004) Mechanism of Ca^{2+} activation of the NADPH oxidase 5 (NOX5). *J. Biol. Chem.* **279**, 18583–18591
9. Grabarek, Z. (2006) Structural basis for diversity of the EF-hand calcium-binding proteins. *J. Mol. Biol.* **359**, 509–525
10. Gifford, J.L., Walsh, M.P., and Vogel, H.J. (2007) Structures and metal-ion-binding properties of the Ca^{2+}-binding helix-loop-helix EF-hand motifs. *Biochem. J.* **405**, 199–221
11. Wong, H.L., Pinontoan, R., Hayashi, K., Tabata, R., Yaeno, T., Hasegawa, K., Kojima, C., Yoshioka, H., Iba, K., Kawasaki, T., and Shimamoto, K. (2007) Regulation of rice NADPH oxidase by binding of Rac GTPase to its N-terminal extension. *Plant Cell* **19**, 4022–4034
12. Banfi, B., Molnar, G., Maturana, A., Steger, K., Hegedus, B., Demaurex, N., and Krause, K.H. (2001) A Ca^{2+}-activated NADPH oxidase in testis, spleen, and lymph nodes. *J. Biol. Chem.* **276**, 37594–37601
13. Shiose, A., Kuroda, J., Tsuruya, K., Hirai, M., Hirakata, H., Naito, S., Hattori, M., Sakaki, Y., and Sumimoto, H. (2001) A novel superoxide-producing NAD(P)H oxidase in kidney. *J. Biol. Chem.* **276**, 1417–1423
14. Ogasawara, Y., Kaya, H., Hiraoka, G., Yumoto, F., Kimura, S., Kadota, Y., Hishinuma, H., Senzaki, E., Yamagoe, S., Nagata, K., Nara, M., Suzuki, K., Tanokura, M., and Kuchitsu, K. (2008) Synergistic activation of the Arabidopsis NADPH oxidase AtrbohD by Ca^{2+} and phosphorylation. *J. Biol. Chem.* **283**, 8885–8892
15. Takeda, S., Gapper, C., Kaya, H., Bell, E., Kuchitsu, K., and Dolan, L. (2008) Local positive feedback regulation determines cell shape in root hair cells. *Science* **319**, 1241–1244
16. Oda, T., Hashimoto, H., Kuwabara, N., Akashi, S., Hayashi, K., Kojima, C., Wong, H.L., Kawasaki, T., Shimamoto, K., Sato, M., and Shimizu, T. (2010) Structure of the N-terminal regulatory domain of a plant NADPH oxidase and its functional implications. *J. Biol. Chem.* **285**, 1435–1445
17. Kuchitsu, K., Kosaka, H., Shiga, T., and Shibuya, N. (1995) EPR evidence for generation of hydroxyl radical triggered by *N*-acetylchitooligosaccharide elicitor and a protein phosphatase inhibitor in suspension-cultured rice cells. *Protoplasma* **188**, 138–142
18. Kawasaki, T., Henmi, K., Ono, E., Hatakeyama, S., Iwano, M., Satoh, H., and Shimamoto, K. (1999) The small GTP-binding protein rac is a regulator of cell death in plants. *Proc. Natl Acad. Sci. USA* **96**, 10922–10926
19. Jagnandan, D., Church, J.E., Banfi, B., Stuehr, D.J., Marrero, M.B., and Fulton, D.J. (2007) Novel mechanism of activation of NADPH oxidase 5. calcium sensitization via phosphorylation. *J. Biol. Chem.* **282**, 6494–6507